SUPPLEMENTARY MATERIALS

Microbial trait multifunctionality drives soil organic matter formation potential

Emily D. Whalen[1,2*], A. Stuart Grandy[1,2], Kevin M. Geyer[3], Eric W. Morrison[1], Serita D. Frey[1,2]

[1]Department of Natural Resources and the Environment, University of New Hampshire, Durham, NH, USA

[2]Center for Soil Biogeochemistry and Microbial Ecology, University of New Hampshire, Durham, NH, USA

[3]Department of Biology, Young Harris College, Young Harris, GA, USA

***Correspondence:** Emily Whalen (ewhalen.cel@gmail.com)

Supplementary Methods and Discussion

Key experimental design decisions and rationale

Pilot experiments to reduce contamination risk: A series of pilot experiments were conducted prior to beginning the final experiment described in this manuscript. The primary goals of the pilot experiments were (1) to ensure that all fungal isolates could be grown in the model soil environment with glucose as a primary C source, and (2) to evaluate methodological approaches that reduced the risk of contamination, such that we could ensure single-species axenic conditions in the full experiment. The greatest risks of contamination occurred during respiration measurements, jar flushing (O_2 replenishment) and substrate amendments. Sterile culturing techniques were used during incubation set-up, and all tools, model soils, incubation containers (jars, specimen cups) and substrate media were autoclaved prior to set-up. All work was conducted within a Laminar flow hood recommended for microbial culturing. Through pilot experiments, we determined that using sterile single-use syringes and needles to make respiration measurements separately for each isolate (different syringe utilized for each grouping of experimental units associated with an isolate on each sampling day) reduced contamination risk. Rather than opening jars to replenish oxygen, jars were flushed using sterile needles fitted with 0.2 μm filters attached to tubes supplying CO_2-free air. The 0.2 μm filters were labeled by species and were re-utilized only for experimental units of the same isolate. Needles (sterile) were replaced between each instance of flushing. Substrate amendments over the course of the long-term incubation experiment (3-6 months) posed a particularly unique challenge to the maintenance of axenic conditions. We developed an approach utilizing a custom 8-inch stainless steel needle that could be fitted to a glass syringe so that substrate amendments could be made

without opening jars. The 8-inch needle was inserted through the rubber ports fitted in the lids of each mason jar, with this particular length being selected such that the needle could reach the bottom of each specimen cup containing model soils. This allowed us to inject the sterilized substrate solution into soils while moving the needle steadily over the vertical length of each soil "core" (50 g cup of soil). The stainless-steel needles and glass syringes were autoclaved (sterilized) prior to substrate amendments.

Based on the results of pilot studies, we decided to establish additional replicates for each isolate to ensure that sufficient replication would remain in case of contamination. A total of eight replicates were established for each isolate. The species that was slowest to establish during initial growth and biomass production, *Panellus stipticus*, was the most challenging taxa to maintain sterile conditions for, with most of the contamination issues occurring during early incubation before *P. stipticus* had established substantial biomass. For this species, we only successfully maintained three experimental units (replicates) under axenic conditions, and therefore were only able to include three replicates in subsequent statistical analyses. For all other isolates, we maintained axenic conditions for at least four replicates, with most species having 5-8 replicates remaining. When > 4 axenic replicates remained, four replicates were selected at random (random number generator) for inclusion in statistical analyses.

Standardization approach based on isolate growth dynamics: Various possible approaches to standardize the timing of substrate amendments and incubation length/harvests were considered in the experimental design phase. An obvious alternative would be to standardize by time[1]. In such a scenario, substrate amendments would be made at the same time for all isolates, and experimental units would be incubated for the same amount of time (e.g., experimental units for all isolates harvested at 3 months). Such an approach would provide insight into differences

in fungal species' contributions to SOM formation and stabilization per unit time, and would be especially relevant if the primary research question was focused on the rate of SOM formation by different fungal isolates. However, the primary aim of our experiment was to evaluate relationships between the trait profiles of fungi and their contributions to different pools of SOM, including relatively stable SOM pools. Had all species been incubated for the same amount of time, it is possible that slower growing species may not have utilized all the added substrate-C, such that unprocessed glucose remained in the soil for some isolates, but not others. This would have (1) biased the measurements of species' contributions to SOM functional pools, especially chemically and biologically stable pools of C, and (2) would have biased our interpretations of trait-SOM relationships. By standardizing by time, it is likely that the traits of fast-growing species with high biomass production would have emerged as important positive predictors of SOM formation (especially stable SOM formation), even if these traits declined in importance over time.

We developed a strategic study design to promote maximum substrate utilization by fungal isolates, such that we could assume a majority of substrate-C had been utilized prior to incubation harvest. We determined the timing of substrate amendments and incubation harvest independently for each isolate. The slowest growing species were incubated for up to ~6 months, whereas the fastest growing species were harvested at ~3 months. Our approach was based on monitoring isolate respiration rates, such that each isolate went through the same pattern of growth dynamics before incubation harvest (described in main text). Based on the maximum respiration rates observed across isolates following substrate amendments, we selected a value of ≤ 1 μg CO_2-C g^{-1} soil $hour^{-1}$ to represent a near-zero respiration rate (see Suppl. Fig. 3). For all fungal isolates included in this study, peak respiration (after substrate amendment) was followed

by declining respiration values, and steady-state growth was determined when isolates exhibited consistently low respiration rates for an extended period of time (≤ 1 μg CO_2-C g^{-1} soil $hour^{-1}$). At this point, it was determined that isolates had utilized a majority of the added substrate-C, and this benchmark was used to determine the timing of the second and third substrate amendments as well as final incubation harvest (on an isolate-specific basis; see main text for additional details).

Alternative approaches to assess complete utilization of the added substrate-C could include: (1) direct measurement of glucose in soils, or (2) measurement of total fungal biomass C at the end of the incubation, and calculation of total C utilization (total respired CO_2-C + fungal biomass C). However, (1) glucose measured in soils at the end of the experiment would not necessarily reflect unutilized substrate-C, as glucose (or other sugars with similar chemical structures) can be exuded by fungi into the soil environment as exudates or metabolites[2]. Secondly, (2) we were unable to estimate total fungal biomass in model soils at the end of the incubation experiment due to challenges with the chloroform fumigation extraction (CFE) method (discussed in main text). Researchers have encountered similar problems with the CFE method in past studies involving model soils [3,4], perhaps due to the high abundance of "clean" mineral surfaces within model soils compared to natural soils. Our strategic experimental design (based on isolate-specific respiration monitoring) thus provided the most robust approach to estimate (near-)complete substrate utilization by fungal isolates while the experiment was in progress, allowing us to determine appropriate timing for substrate additions and to assume a majority of the added substrate-C had been utilized prior to incubation harvest.

Choice of glucose as a primary C source: While multiple C-supplying substrates were considered for use in this experiment, we ultimately decided to include glucose as the primary C

source (90% of C; other 10% supplied by potato dextrose infusion). Glucose has been used in numerous studies as a model substrate and has been shown to be rapidly assimilated and metabolized by a wide range of microbial taxa[2], including saprotrophic fungi[5]. A key aspect of our experimental design was the strategic timing of substrate additions and harvests to promote complete utilization of substrate-C. Compared to other C-supplying substrates, glucose exhibits low levels of discrimination among microbial taxa[6]. While more complex substrates (e.g., cellulose) were considered, glucose is water-soluble and therefore could be applied more evenly and homogenously throughout the soil as a liquid solution (autoclaved/sterilized). Together, these decisions guided our selection of glucose as a primary C-supplying substrate.

Substrate stoichiometry and carbon application rate: The C:N ratio of the substrate media used in this experiment was similar to soil C:N values observed at the site where fungal cultures were isolated, the Harvard Forest (C:N range from ~16-27 for mineral soils[7]). We chose a C:N ratio of 20:1 specifically, as it was expected to alleviate N limitation for fungal isolates[8,9], whose average biomass C:N ratio was ~10 (described in[10]). A total of three substrate amendments (1 ml each; 5.6 mg C g^{-1} soil) were applied over the course of the incubation. Each experimental unit contained 50 g soil, and thus 240 mg C were added per substrate amendment. The rate of C application was selected to (1) minimize the total number of substrate additions required (lowering contamination risk) and (2) prevent osmotic shock to fungal isolates (a concern with highly concentrated glucose solutions). At the end of the experiment, a total of 840 mg C had been added to each experimental unit. We selected this amount of C as a sufficient stopping point for our experiment, because it was expected to increase soil C concentrations into a range comparable to the C content of agricultural mineral soils (0.8-1.0% C). While this range is low compared to more C-rich forest or grassland soils, it is still a realistic range of total C values

observed among natural field soils, and it allowed us to end the incubations after ~3-6 months (depending on isolate). As discussed in the main text, a central constraint of our study was the need to maintain axenic conditions of fungal cultures. Because the risk of contamination increases with duration of incubation and number of substrate amendments, we decided that three substrate additions (840 mg C) would be sufficient to observe and compare differences in SOM formation across fungal isolates.

Multiple approaches to quantify isolate CUE: Given that carbon use efficiency (CUE) measurements can vary based on isolate growth stage and resource availability (e.g., C uptake from glucose vs. biomass recycling), we decided to include three separate metrics of CUE in our analysis of trait-SOM relationships. The three metrics were as follows: CUE measured during log-phase growth in (1) liquid culture and (2) model soils (both calculated as CUE = $\frac{mass\ specific\ growth\ rate\ (\mu)}{(\mu + mass\ specific\ growth\ rate\ (Rmass))}$), and (3) CUE measured at stationary growth in model soils (calculated as CUE = $\frac{^{18}MBC}{^{18}MBC + cumulative\ CO_2{-}C\ respired}$) (additional details provided in main text Methods). Liquid culture values, previously published by Morrison et al.[10], were collected from short-term incubations (~1 week to 1 month, depending on isolate) where respiration and biomass measurements were made at regular intervals. These values are included as a representation of fungal isolates' maximum CUE under optimal growth conditions. Values ranged from 0.33 ± 0.03 to 0.72 ± 0.08, consistent with previous studies of pure microbial cultures grown on non-limiting supplies of glucose (0.4-0.88), which can approach theoretical maxima[11]. The CUEs of fungal isolates in model soils (assessed during log-phase growth) were measured in short-term incubations mirroring the liquid culture approach. Soil CUE (log-phase) values were lower on average than liquid culture measurements, ranging from 0.21 ± 0.03 to

0.60 ± 0.02. These values are more similar to CUE values observed for soil microbial communities (0.24-0.77)[11], which tend to be lower than maximal values observed in liquid culture, in part because soil properties can limit substrate availability and C uptake rates (e.g., via temporary mineral sorption or occlusion within pore spaces). Both the liquid culture and soil CUE measurements made during log-phase growth are expected to capture CUE before significant biomass turnover begins[12], which is known to influence CUE[11]. The third metric of CUE, assessed in model soils during stationary growth, integrates this effect of biomass turnover. This measure of CUE (measured via ^{18}O-water incorporation into DNA) captures both the efficiency of substrate retention as fungal biomass, as well as the efficiency of biomass recycling across generations of fungal cells[11]. Interestingly, soil CUE at stationary growth ranged from 0.46 ± 0.04 to 0.96 ± 0.01, making it the highest of the three CUE measurements (on average). While past studies have shown that biomass turnover and substrate recycling can reduce CUE values for mixed soil microbial communities, especially if microbial necromass becomes incorporated into temporarily inaccessible SOM pools[11], relatively high CUE values observed in our experiment for some isolates could be indicative of more "self-sustaining" fungal populations that efficiently recycle (in this case, their own) biomass C. We may have been more likely to observe this pattern in our experiment (compared to natural field soils) because of the high levels of biomass production per unit area (visible to the naked eye and under a microscope), which likely represented a large pool of substrate available for fungal recycling.

Because each individual metric of CUE is unlikely to represent the long-term CUE dynamics of fungal isolates on its own, we calculated an average value that integrates the three metrics to better approximate mean CUE of fungal isolates over the course of the long-term incubations. These values are integrated into certain analyses presented in the main text (e.g.,

Fig. 1; Fig. 4). In addition, we presented each of the three CUE metrics separately in analyses examining relationships between fungal traits and SOM formation (e.g., PLSR, Fig. 4) such that readers could assess these relationships individually for each CUE measure x SOM pool combination.

Supplementary Tables and Figures

Supplementary Table 1. Average trait values (standard error in parentheses) observed at the phylum-level for Basidiomycota, Ascomycota, and Mucoromycotina. One-way ANOVA (parametric) or Kruskal-Wallis (non-parametric) results are presented for each trait and associated post-hoc comparisons are presented when ANOVA or Kruskal-Wallis results were significant (Tukey HSD for parametric data; Dunn test for non-parametric data). Optimum growth rate (GR) and CUE were conducted in liquid culture during log-phase growth. Soil growth rate and CUE measurements were conducted during log-phase growth unless specified at stationary phase growth. Units are as follows for each trait measurement: growth rate (μg biomass-C produced biomass-C^{-1} hr^{-1}), turnover (days), hyphal length (m hyphae g^{-1} dry soil), hyphal surface area (m^2 g^{-1} dry soil), hyphal diameter (μm), melanin (mg g^{-1} biomass), proteins and other compounds measured by Py-GC/MS (% relative abundance in biomass), potential enzyme activities (μmol substrate h^{-1} g^{-1} dry soil).

	Phyla			*ANOVA/ Kruskal*	*Post-hoc Tukey HSD/Dunn*		
Variable	**Basidiomycota (n=8)**	**Ascomycota (n=20)**	**Mucoromycotina (n=8)**	**(P-values)**	**Basidio-Asco**	**Asco-Mucor**	**Mucor-Basidio**
Optimum GR	0.006 (0.001)	0.015 (0.001)	0.080 (0.008)	<0.001***	0.007**	0.002**	<0.001***
Soil GR	0.004 (0.0003)	0.023 (0.004)	0.042 (0.009)	<0.001***	0.003**	0.033*	<0.001***
Optimum CUE	0.677 (0.04)	0.568 (0.04)	0.461 (0.03)	0.011*	0.117	0.011*	0.002*
Soil CUE	0.419 (0.08)	0.491 (0.03)	0.304 (0.047)	0.034*	0.537	0.027*	0.345
Soil CUE (stationary)	0.726 (0.09)	0.781 (0.04)	0.495 (0.03)	0.019*	0.364	0.003*	0.021*
Turnover	1.408 (0.83)	0.900 (0.23)	1.433 (0.17)	0.246	-	-	-
BG + CBH	964.1 (343.1)	5271 (581.4)	842.2 (304.0)	<0.001***	<0.001***	<0.001***	0.399
PHOS	436.1 (124.2)	1553 (219.7)	1889 (233.3)	0.012*	0.006**	0.197	0.003**
NAG	1580 (264.1)	1959 (412.4)	894.5 (368.9)	0.292	-	-	-
LAP	0.00 (0.00)	909.7 (615.6)	0.00 (0.00)	0.097	-	-	-
OX	43.43 (13.4)	10.09 (1.15)	6.536 (1.84)	0.002**	0.003**	0.081	<0.001***
Hyphal SA	76.36 (23.1)	133.6 (22.0)	784.2 (50.0)	<0.001***	0.137	<0.001***	<0.001***
Hyphal length	17.31 (6.22)	12.90 (1.55)	17.50 (1.83)	0.413	-	-	-
Hyphal diam.	1.535 (0.14)	2.634 (0.25)	15.69 (2.24)	<0.001***	0.014*	0.002*	<0.001***
Melanin	0.038 (0.001)	0.036 (0.005)	0.008 (0.003)	<0.001***	0.214	<0.001***	<0.001***
Phenols	5.481 (0.399)	7.108 (0.413)	10.78 (1.069)	<0.001***	0.159	<0.001***	<0.001***
Proteins	6.809 (0.316)	10.71 (0.709)	11.80 (0.973)	0.005**	0.002**	0.241	0.002**
N-bearing	8.937 (0.831)	11.06 (0.812)	14.23 (0.111)	0.022*	0.087	0.028*	0.003**
Polysacc.	32.07 (1.961)	36.81 (1.123)	29.28 (2.105)	0.020*	0.044*	0.005**	0.222
Lipids	35.62 (2.723)	17.99 (1.621)	16.56 (6.077)	0.003**	<0.001***	0.486	0.004*
Aromatics	2.246 (0.281)	3.043 (0.236)	2.926 (0.296)	0.158	-	-	-

Supplementary Table 2. Average contributions to SOM pools (standard error in parentheses) observed at the phylum-level for Basidiomycota, Ascomycota, and Mucoromycotina. *P*-values from one-way ANOVA (parametric) or Kruskal-Wallis (non-parametric) results are presented for each SOM pool and associated post-hoc comparisons are presented when ANOVA or Kruskal-Wallis results were significant (Tukey HSD for parametric data; Dunn test for non-parametric data).

	Phyla			***ANOVA/ Kruskal***	***Post-hoc Tukey HSD/Dunn***		
Variable	**Basidiomycota (n=8)**	**Ascomycota (n=20)**	**Mucoromycotina (n=8)**	**(P-values)**	**Basidio-Asco**	**Asco-Mucor**	**Mucor-Basidio**
Total C (%)	0.730 (0.03)	0.695 (0.03)	0.641 (0.03)	0.301	-	-	-
MAOM-C (%)	1.65 (0.16)	1.47 (0.07)	1.26 (0.06)	0.045*	0.425	0.278	0.041*
POM-C (%)	0.08 (0.006)	0.285 (0.02)	0.238 (0.02)	<0.001***	<0.001***	0.416	0.004**
Water-stable aggregates (%)	80.21 (1.60)	83.13 (1.11)	61.6 (1.20)	<0.001***	0.133	<0.001***	0.003**
Chemically stable C (%)	22.59 (5.46)	54.38 (2.04)	46.45 (2.61)	<0.001***	<0.001***	0.044*	0.032*
Biologically stable C (%)	55.25 (4.17)	69.68 (2.61)	71.69 (1.79)	0.012*	0.004**	0.303	0.003*

Supplementary Table 3. Full PLSR model outputs for three separate iterations of PLSR on the randomized dataset (three randomizations). (A) Results for total C, POM-C and MAOM-C. (B) Results for chemically-stable C, biologically-stable C and water-stable aggregates. Three iterations of PLSR were conducted for each SOM functional pool. The five variables with the highest loadings on PLSR factor 1 and factor 2 are presented for each model, with the X loading value and VIP scores presented in parentheses. Average values were calculated across the three randomizations for the main text (Fig. 4).

A

Randomization # →	**Randomization 1**		**Randomization 2**		**Randomization 3**	
Response (Y)	**Model info**	**Variable (loading/VIP)**	**Model info**	**Variable (loading/VIP)**	**Model info**	**Variable (loading/VIP)**
Total C	Two factor model (cumulative R^2Y = 69.2%): -F1: 56.8% -F2: 12.4%	Factor 1 (56.8%): CUE soil, ^{18}O (0.40/1.80) Growth rate, opti. (-0.31/1.08) Biomass polysacc (0.29/1.36) Growth rate, soil (-0.29/1.19) BG (0.28/1.06) Factor 2 (12.4%): Hyphal SA (0.37/0.89) NAG (-0.35/1.34) Biomass phenol (0.34/0.80) Hyphal length (0.30/1.73) Melanin (-0.30/0.76)	Two factor model (cumulative R^2Y = 66.9%): -F1: 47.7% -F2: 19.2%	Factor 1 (47.7%): CUE soil, ^{18}O (0.39/1.88) Growth rate, opti. (-0.32/1.13) Growth rate, soil (-0.29/1.17) Hyphal SA (-0.29/1.04) BG (0.28/1.05) Factor 2 (19.2%): NAG (-0.40/1.48) Phenol (0.32/1.02) Hyphal SA (0.31/1.03) Melanin (-0.30/0.81) PHOS (0.29/0.81)	Two factor model (cumulative R^2Y = 69.3%): -F1: 47.7% -F2: 21.6%	Factor 1 (47.7%): CUE soil, ^{18}O (0.38/1.69) Growth rate, opti. (-0.33/1.16) Hyphal SA (-0.30/1.05) Growth rate, soil (-0.29/1.19) BG (0.28/1.01) Factor 2 (21.6%): NAG (-0.42/1.77) Phenol (0.36/1.13) Melanin (-0.34/0.95) Hyphal SA (0.29/1.06) Lipid (-0.29/0.38)
POM-C	Two factor model (cumulative R^2Y = 70.1%): -F1: 65.3% -F2: 4.9%	Factor 1 (65.3%): Biomass lipid (-0.37/1.56) CBH (0.35/2.01) ABTS (-0.35/1.48) PHOS (0.30/1.47) Biomass polysacc (0.29/1.66) Factor 2 (4.9%): Biomass phenol (-0.32/0.57) BG (0.30/1.60) Biomass protein (-0.30/0.88) CBH (0.29/2.01) CUE soil, ^{18}O (0.29/0.73)	Two factor model (cumulative R^2Y = 68.8%): -F1: 64.3% -F2: 4.5%	Factor 1 (64.3%): Biomass lipid (-0.37/1.58) CBH (0.36/2.08) ABTS (-0.34/1.49) PHOS (0.31/1.48) BG (0.30/1.70) Factor 2 (4.5%): Biomass protein (-0.33/0.96) Biomass N-bearing (-0.32/0.53) Biomass phenol (-0.31/0.63) CUE soil, ^{18}O (0.31/0.77) CBH (0.30/2.08)	Two factor model (cumulative R^2Y = 69.8%): -F1: 64.8% -F2: 5.0%	Factor 1 (64.8%): CBH (0.37/2.01) Biomass lipid (-0.37/1.57) ABTS (-0.34/1.41) BG (0.32/1.60) PHOS (0.30/1.55) Factor 2 (5.0%): Biomass protein (-0.39/0.92) Biomass phenol (-0.32/0.50) Biomass N-bearing (-0.31/0.54) CBH (0.31/2.01) CUE soil, ^{18}O (0.29/0.86)
MAOM-C	Two factor model (cumulative R^2Y = 90.4%): -F1: 74.4% -F2: 16.0%	Factor 1 (74.4%) CUE soil, ^{18}O (0.37/1.50) Growth rate, opti. (-0.30/1.06) CUE optimum (0.30/1.40) Biomass polysacc (0.29/1.27) Biomass N-bear (-0.28/1.05) Factor 2 (16.0%) Melanin (-0.37/0.65) NAG (-0.35/1.35) Hyphal SA (0.34/0.77) Biomass phenol (0.31/0.81) Hyphal length (0.27/1.95)	Two factor model (cumulative R^2Y = 90.8%) -F1: 62.4% -F2: 22.8% -F3: 5.5%	Factor 1 (62.4%) CUE soil, ^{18}O (0.35/1.63) Growth rate, opti. (-0.33/1.12) CUE optimum (0.30/1.43) Biomass polysacc (0.29/1.23) Biomass N-bear (-0.29/1.16) Factor 2 (22.8%) Melanin (-0.41/0.89) NAG (-0.40/1.44) Hyphal SA (0.29/0.96) Biomass phenol (0.30/0.94) BG (-0.28/0.72)	Two factor model (cumulative R^2Y = 89.7%): -F1: 63.3% -F2: 20.5% -F3: 5.9%	Factor 1 (63.3%) CUE soil, ^{18}O (0.35/1.47) Growth rate, opti. (-0.32/1.12) CUE optimum (0.30/1.33) Biomass N-bear (-0.30/1.26) Biomass polysacc (0.28/1.16) Factor 2 (20.5%) Melanin (-0.40/0.88) NAG (-0.38/1.57) Hyphal SA (0.29/0.94) Biomass phenol (0.29/0.92) BG (-0.28/0.75)

B

Chemically stable C	Two factor model (cumulative R^2Y = 93.6%): -F1: 78.0% -F2: 8.9% -F3: 6.5%	Factor 1 (78.0%) Biomass lipid (-0.38/1.67) Biomass protein (0.34/1.53) ABTS (-0.32/1.47) TMB (-0.31/1.16) Biomass phenol (0.28/1.03) Growth rate, soil (0.26/1.11)	Two factor model (cumulative R^2Y = 92.5%): -F1: 75.1% -F2: 9.7% -F3: 7.7%	Factor 1 (75.1%) Biomass lipid (-0.38/1.54) Biomass protein (0.35/1.44) ABTS (-0.30/1.17) TMB (-0.30/1.04) Biomass phenol (0.27/1.04) Growth rate, soil (0.27/1.14)	Two factor model (cumulative R^2Y = 88.3%): -F1: 79.6% -F2: 8.7%	Factor 1 (79.6%) Biomass lipid (-0.38/1.58) Biomass protein (0.35/1.57) ABTS (-0.32/1.66) TMB (-0.31/1.18) PHOS (0.29/1.37) Biomass phenol (0.28/1.10)
		Factor 2 (8.9%) BG (0.36/1.07) Growth rate, opti. (-0.36/0.60) CUE soil, ^{18}O (0.35/0.51) Biomass polysacc (0.33/1.09) Hyphal SA (-0.33/0.64)		Factor 2 (9.7%) BG (0.35/1.11) Growth rate, opti. (-0.35/0.59) CUE soil, ^{18}O (0.33/0.54) Biomass polysacc (0.28/0.96) Hyphal SA (-0.38/0.54)		Factor 2 (8.7%) BG (0.35/1.00) Growth rate, opti. (-0.35/0.55) CUE soil, ^{18}O (0.33/0.41) Biomass polysacc (0.29/0.80) Hyphal SA (-0.37/0.55)
Biologically stable C	Two factor model (cumulative R^2Y = 68.6%): -F1: 47.5% -F2: 21.1%	Factor 1 (47.5%) Biomass protein (0.35/1.73) Biomass phenol (0.33/1.17) Growth rate, soil (0.31/1.26) TMB (-0.28/1.18) Biomass N-bear. (0.27/1.14)	Two factor model (cumulative R^2Y = 63.8%): -F1: 40.1% -F2: 12.0% -F3: 11.8%	Factor 1 (40.1%) Biomass protein (0.37/1.42) Biomass phenol (0.33/1.03) Growth rate, soil (0.31/1.20) Biomass lipid (-0.31/1.15) Biomass N-bear. (0.27/1.09)	Two factor model (cumulative R^2Y = 64.4%): -F1: 43.5% -F2: 21.0%	Factor 1 (43.5%) Biomass protein (0.35/1.73) Biomass phenol (0.33/1.16) Biomass lipid (-0.32/1.39) Growth rate, soil (0.29/1.35) Biomass N-bear. (0.28/1.08)
		Factor 2 (21.1%) BG (0.39/0.58) Hyphal SA (-0.37/0.98) Growth rate, opti.(-0.31, 0.96) CUE soil, ^{18}O (0.29/0.76) CUE soil (0.27/1.05)		Factor 2 (12.0%) BG (0.42/1.00) Hyphal SA (-0.39/0.91) Growth rate, opti. (-0.32, 0.93) Hyphal length (-0.32/1.37) CUE soil, ^{18}O (0.28/1.14)		Factor 2 (21.0%) BG (0.41/0.90) Growth rate, opti. (-0.30, 0.93) CUE soil, ^{18}O (0.35/0.80) CUE soil (0.32/1.23) Biomass polysacc (0.29/0.90)
Water-stable aggregates	Two factor model (cumulative R^2Y = 89.6%): -F1: 75.9% -F2: 13.6%	Factor 1 (75.9%) Growth rate, opti. (-0.36/1.72) Hyphal SA (-0.34/1.59) CUE soil, ^{18}O (0.33/1.34) Biomass phenol (-0.29/1.13) BG (0.27/1.22)	Two factor model (cumulative R^2Y = 89.0%): -F1: 78.4% -F2: 10.6%	Factor 1 (75.9%) Growth rate, opti. (-0.37/1.73) Hyphal SA (-0.37/1.81) CUE soil, ^{18}O (0.32/1.36) Biomass phenol (-0.29/1.22) BG (0.29/1.28)	Two factor model (cumulative R^2Y = 87.7%): -F1: 75.2% -F2: 12.5%	Factor 1 (75.9%) Growth rate, opti. (-0.37/1.69) Hyphal SA (-0.37/1.83) CUE soil, ^{18}O (0.32/1.40) Biomass phenol (-0.29/1.19) BG (0.28/1.23)
		Factor 2 (13.6%) CUE, soil (0.38/0.94) PHOS (0.32/0.45) LAP (0.31/0.52) ABTS (-0.30/0.64) Growth rate, opti. (0.29/0.99)		Factor 2 (13.6%) CUE, soil (0.30/0.94) PHOS (0.33/0.49) LAP (0.33/0.64) Growth rate, soil (0.31/1.46) Biomass protein (0.30/0.68)		Factor 2 (13.6%) CUE, soil (0.32/1.55) PHOS (0.34/0.52) LAP (0.34/0.69) Growth rate, soil (0.32/0.94) Biomass protein (0.29/0.72)

Supplementary Figure 1. Boxplots showing all measured traits and their relative expression across fungal species. Boxplots represent 25th and 75th percentile, median and outlying points. Whiskers extend from minimum to maximum values (no further than 1.5x the inter-quartile range). Colors represent fungal species. Results (p-values) are presented for one-way ANOVA or Kruskal-Wallis analyses on the effect of species on each trait measurement (n=4, except for *P. stipticus*, n=3). Optimum growth rate (GR) and CUE were conducted in liquid culture during log-phase growth. Soil growth rate and CUE measurements were conducted during either log-phase or stationary phase growth, as specified in the axis titles. Units are as follows for each trait measurement: growth rate (μg biomass-C produced biomass-C^{-1} hr^{-1}), turnover (days), hyphal length (m hyphae g^{-1} dry soil), hyphal surface area (m^2 g^{-1} dry soil), hyphal

diameter (µm), melanin (mg g^{-1} biomass), proteins and other compounds measured by Py-GC/MS (% relative abundance in biomass), potential enzyme activities (µmol substrate h^{-1} g^{-1} dry soil). For *H. minutispora*, samples were separately categorized as sporulating (S) or non-sporulating (N). Source data are provided as a Source Data file.

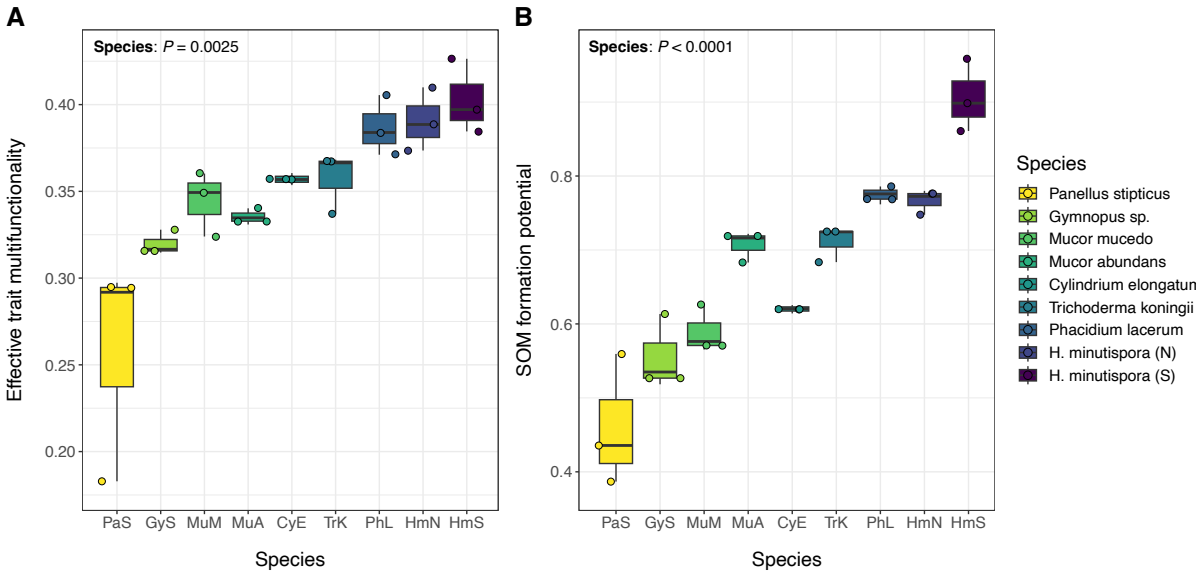

Supplementary Figure 2. Boxplots of effective trait multifunctionality (A) and SOM formation potential (B) across fungal species. Boxplots represent 25th and 75th percentile, median and outlying points. Whiskers extend from minimum to maximum values (no further than 1.5x the inter-quartile range). Colors represent fungal species. Source data are provided as a Source Data file.

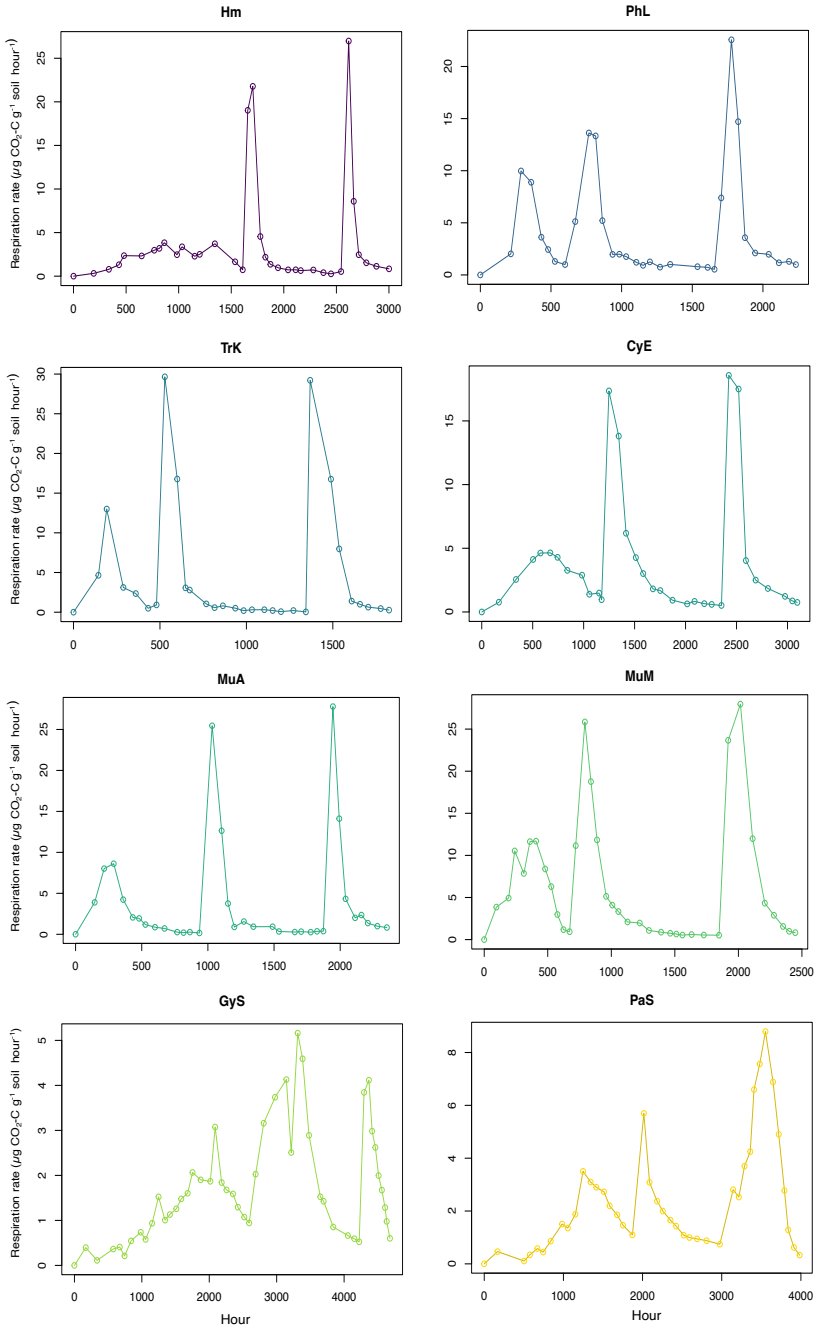

Supplementary Figure 3. Average respiration rates observed for each fungal species over the course of the long-term incubation. Colors represent different fungal species (n=3). Respiration rates were monitored to determine the timing of the second and third substrate additions and final incubation harvests on an isolate-specific basis. The second substrate amendment was added once an isolate's respiration rate dropped to ≤ 1 μg CO_2-C g^{-1} soil $hour^{-1}$. The third substrate amendment was added after isolates had undergone a period of stationary growth for ~20 days (500 hours), which was determined to begin when each isolate's respiration

rate reached ≤ 1 µg CO_2-C g^{-1} soil $hour^{-1}$. This period of stationary growth was intentionally induced to promote fungal biomass recycling. After the third substrate addition, isolates underwent an exponential growth phase, followed by a period of declining growth. Final incubation harvests were made once an isolate's respiration rate had once again declined to < 1 µg CO_2-C g^{-1} soil $hour^{-1}$.

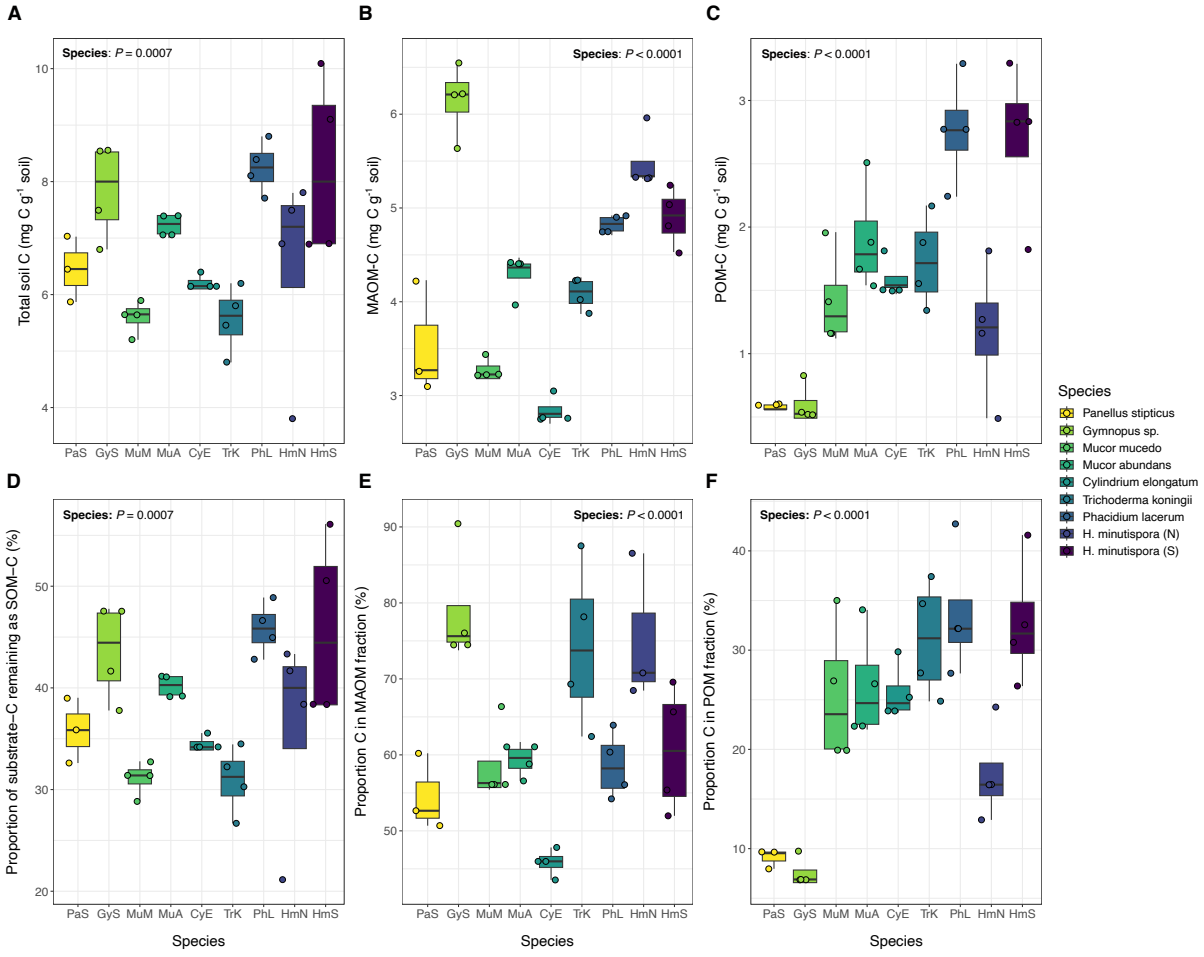

Supplementary Figure 4. Carbon concentrations and proportions of remaining soil C comprised by different SOM pools. Total soil C concentrations (mg C g^{-1} soil) of bulk soils (A), and C concentrations within MAOM and POM fractions (mg C g^{-1} soil) (B-C). Proportion (%) of total substrate C added over the course of the long-term experiment that remained as SOM-C (panel D); (E) proportion of total soil C (measured by combustion analysis at end of incubation, panel A) that was present in the MAOM fraction, compared with the POM fraction (F). Box colors represent individual fungal species (n=4). Individual sample points are shown as dot plots. Boxplots represent 25th and 75th percentile, median and outlying points. Whiskers extend from minimum to maximum values (no further than 1.5x the inter-quartile range). Source data are provided as a Source Data file.

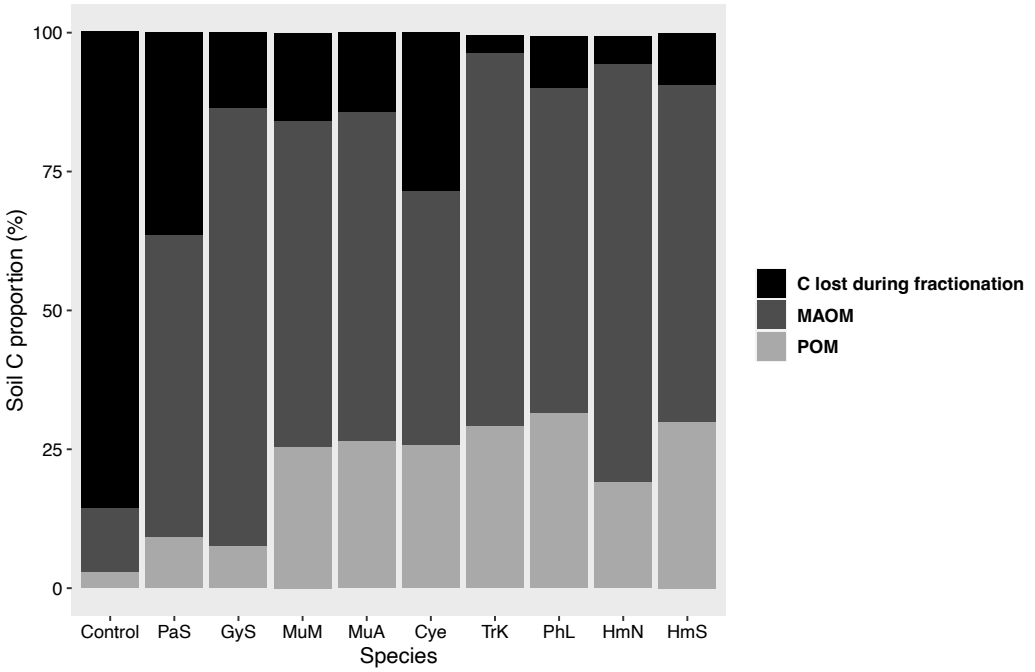

Supplementary Figure 5. Proportion (%) of total soil C comprised by the MAOM and POM fractions, alongside C lost during fractionation across fungal species (n=4). Carbon loss was calculated by subtracting the C concentrations of the MAOM and POM fractions (mg C g^{-1} soil) from total soil C concentrations (measured by combustion analysis; mg C g^{-1} soil). Overall, a much higher proportion of C was lost during fractionation for control soils (model soils + substrate; no fungi) than for model soils incubated with fungal isolates. Carbon loss during fractionation may have occurred due to desorption of MAOM, release of organic matter formerly occluded within the POM fraction or DOC mobilization during the 18h shaking period with sodium hexametaphosphate (standard dispersion protocol prior to wet sieving; see Methods in main text). After dispersion, soils were sieved to separate the < 53 μm fraction (MAOM) from the > 53 μm fraction (POM). Soil suspensions/solutions were then centrifuged and the supernatant was carefully decanted to isolate the MAOM and POM fractions. Carbon lost during fractionation represents the amount of C that was removed with the supernatant (not remaining in the MAOM or POM fractions). Source data are provided as a Source Data file.

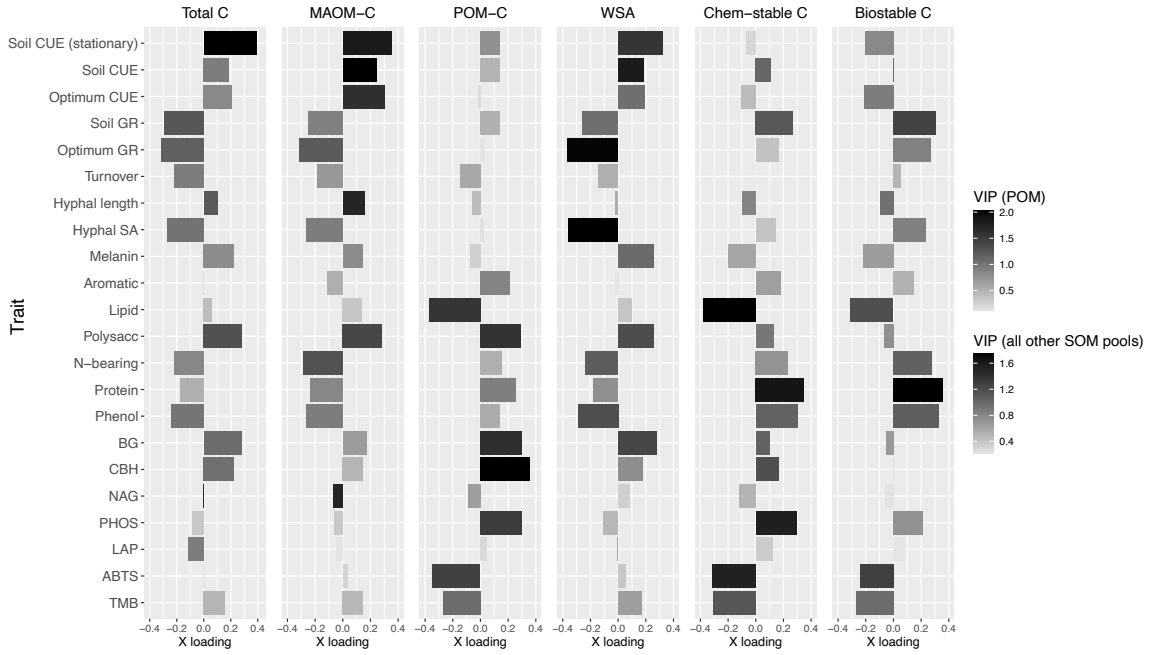

Supplementary Figure 6. Bar plots of trait loadings on the first (most explanatory) PLSR latent factor for each SOM functional pool, accounting for 50-78% of variation in each pool. From left to right: total C, MAOM-C, POM-C, water-stable aggregates (WSA), chemically stable C, and biologically stable C (n=3). This figure corresponds with Fig. 4 in the main text and includes an additional SOM functional pool (POM). X loadings are presented along the x axis, and bar color is shaded to represent variable importance scores (VIP) for each trait variable, indicating the overall importance of each trait to the PLSR model, integrating latent factor 2, and in some cases, factor 3. Full PLSR model outputs are available in Supplementary Table 1.

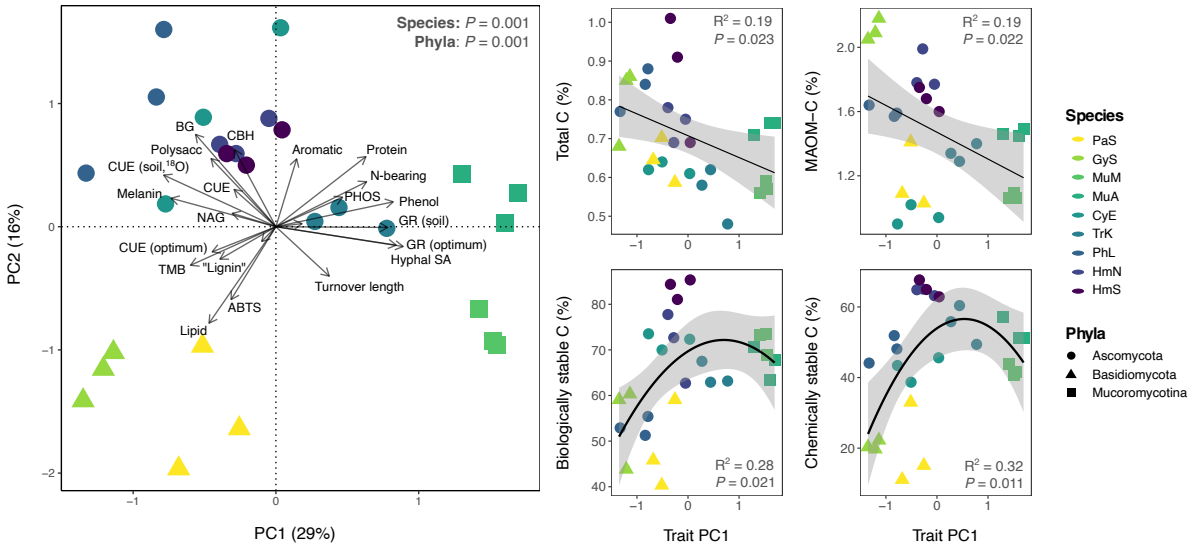

Supplementary Figure 7. Principal components analysis (PCA) of fungal trait profiles, with the two most explanatory PC axes explaining 45% of variation in fungal trait data. This figure corresponds with Fig. 2 in the main text and includes additional correlation plots for PC axis 1 versus four different SOM functional pools: total C, MAOM-C, biologically stable C and chemically stable C (n=3). Sample point color represents fungal species, while point shape represents fungal phyla. P-values and R^2 are presented for the polynomial regression model with the lowest mean square error for each SOM functional pool. Error bands represent 95% confidence interval. Source data are provided as a Source Data file.

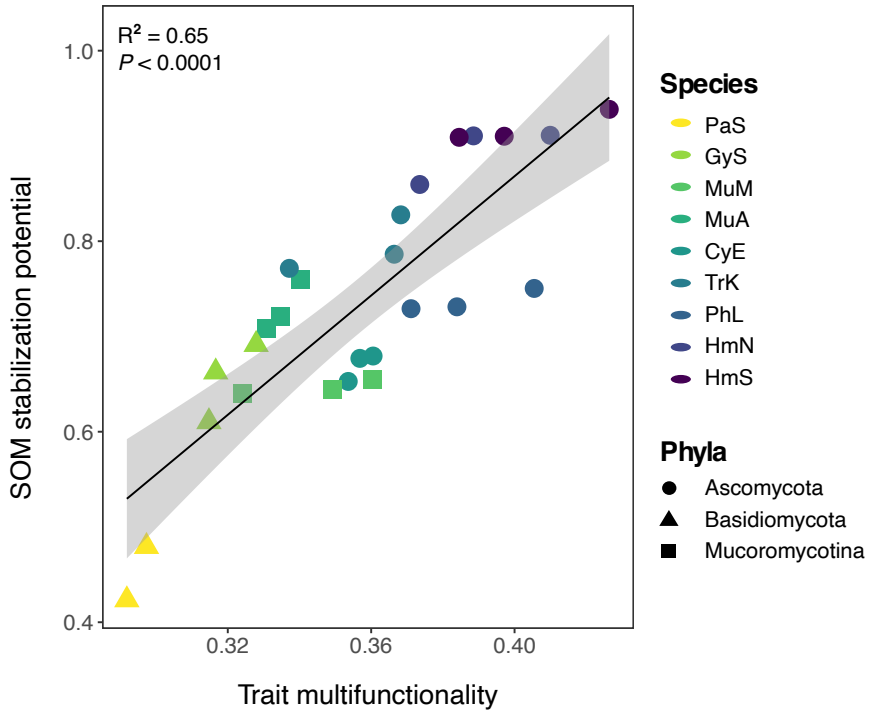

Supplementary Figure 8. Linear regression between trait multifunctionality and SOM stabilization potential (multifunctionality), which included only those SOM functional pools that are putatively stable (MAOM-C, water-stable aggregates, biologically stable C, chemically stable C) (n=3). Point color represents fungal species, while point shape represents fungal phyla. One PaS replicate with significantly lower trait multifunctionality (~0.2) is removed from the plot for ease of visualizing differences across other samples, but does not change the interpretation of the results (both $P < 0.0001$). ANOVA results are presented for the model that included all replicates ($R^2 = 0.65$; $P < 0.0001$). Error bands represent 95% confidence interval. Source data are available as a Source Data file.

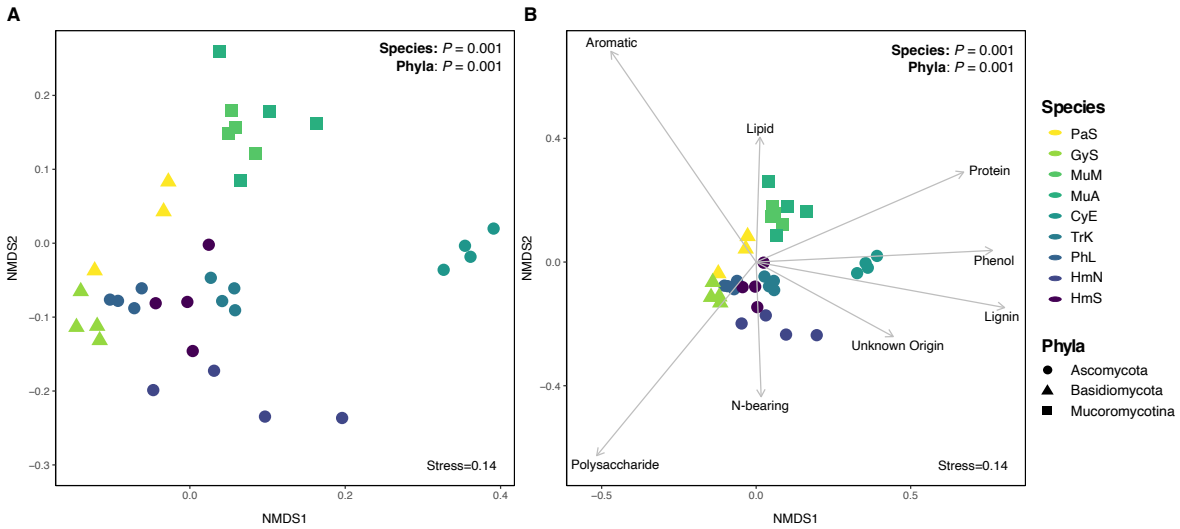

Supplementary Figure 9. NMDS ordination of MAOM chemical composition (individual compound-level dataset) after long-term incubation with fungal isolates (n=4), without environmental vectors (A) or with significant ($P < 0.05$) environmental vectors (B) representing broad chemical compound classes. Version without environmental vectors (A) is included for ease of visualizing differences across samples. Sample point color represents fungal species, while point shape represents fungal phyla. Results of PERMANOVA analyses for both species and phyla are included.

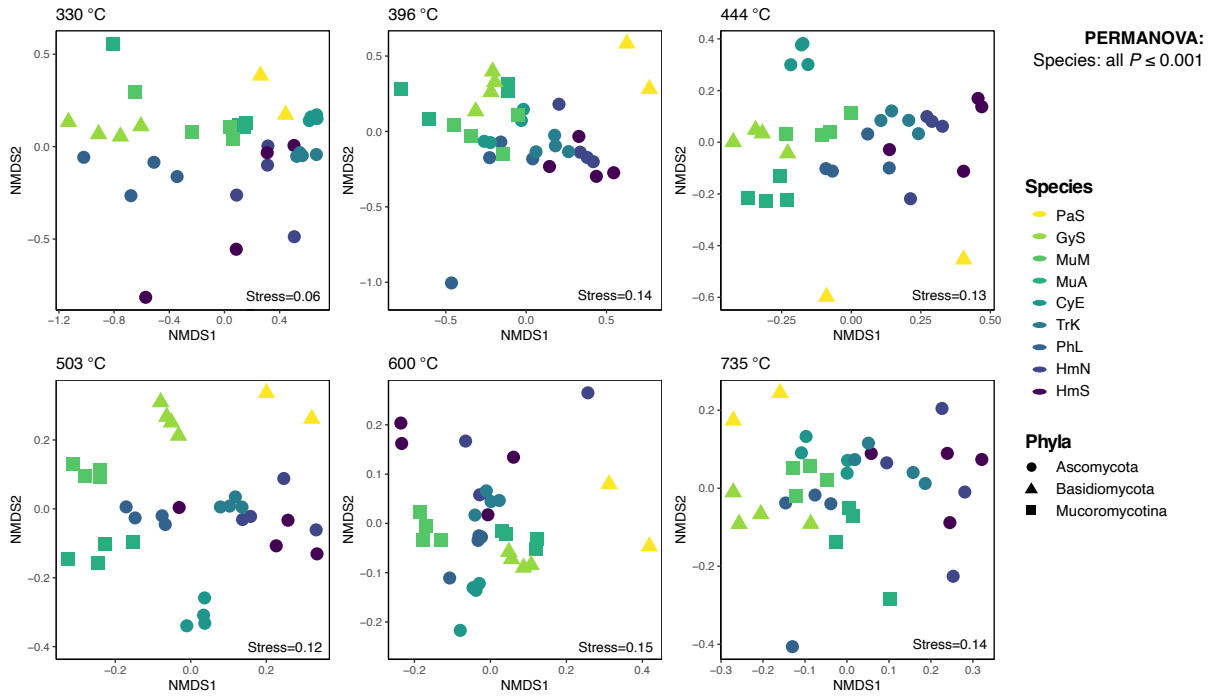

Supplementary Figure 10. NMDS ordinations of SOM chemical composition after long-term incubation with fungal isolates (n=4). Separate panels are shown for each pyrolysis thermal fraction (ramped pyrolysis GC/MS approach), 330ºC-735ºC. Significant variation in species' SOM chemistries were observed for each thermal fraction (all $P \leq 0.001$; PERMANOVA). Point color represents fungal species, while point shape represents fungal phyla.

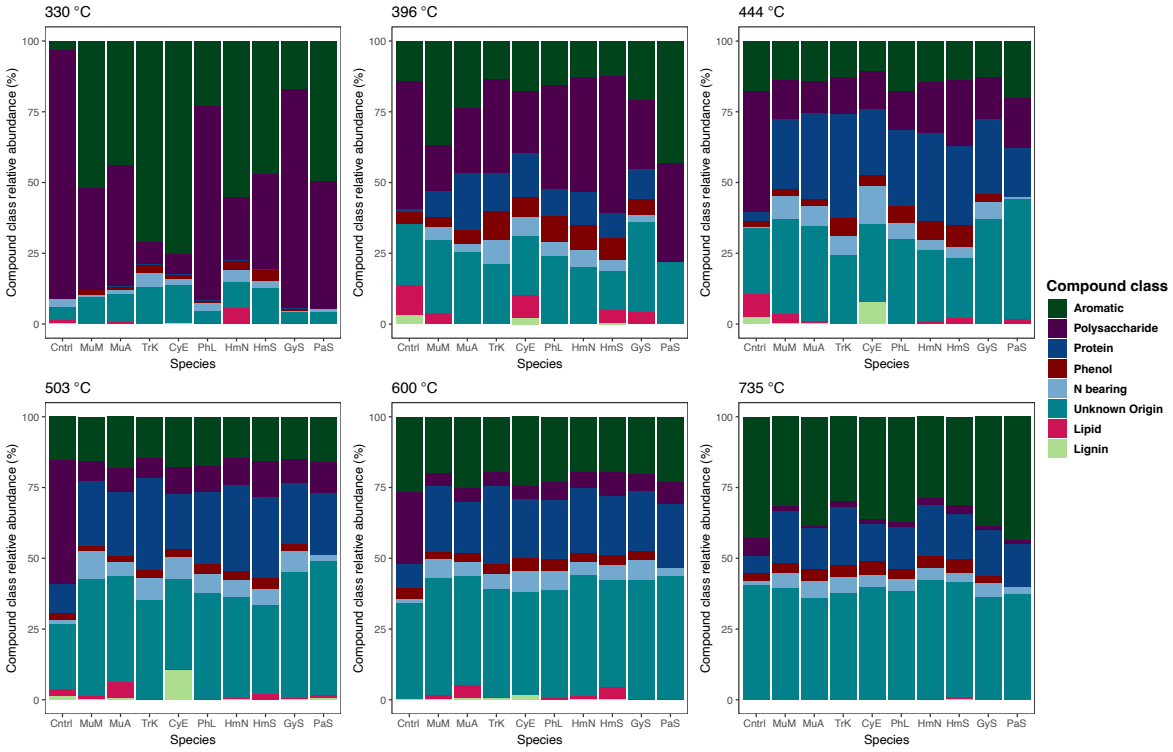

Supplementary Figure 11. Stacked bar plots showing SOM chemical composition after long-term incubation with fungal isolates (n=4), with a separate panel for each pyrolysis thermal fraction (ramped pyrolysis GC/MS approach; 330ºC-735ºC). Bar segment color represents the relative abundance (%) of broad chemical compound classes (aromatics, polysaccharides, proteins, phenols, N-bearing compounds, lipids, "lignin" and unknown origin). "Lignin" is hypothesized to represent fungal-derived melanins and may have been misidentified by Py-GC/MS analysis of the model soils. This figure corresponds with the NMDS plots presented in Supplementary Figure 8.

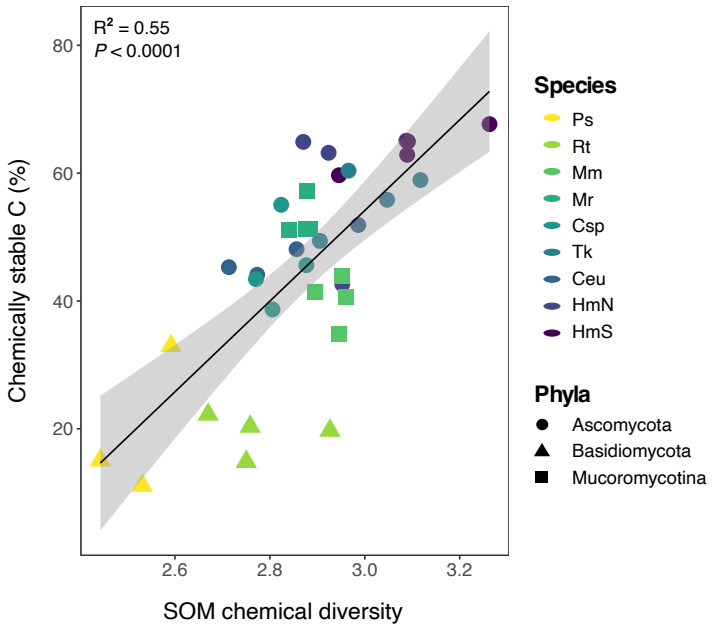

Supplementary Figure 12. Chemical diversity of thermally stable SOM (735°C) versus the proportion of chemically stable SOM produced by fungal species. Chemical diversity was calculated using the index for Shannon diversity (n=4). Sample point color represents fungal species, while point shape represents fungal phyla. One-way ANOVA results are presented (R^2 = 0.55; $P < 0.0001$). Error band represents 95% confidence interval. Source data are available as a Source Data file.

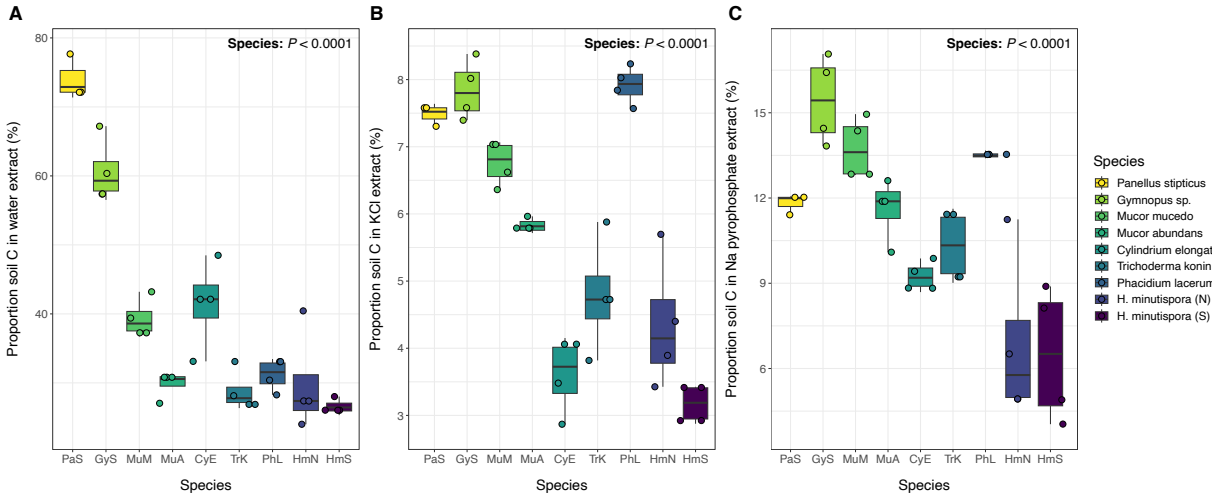

Supplementary Figure 13. **Proportion of fungal-derived SOM-C extracted by (A) water, (B) KCl, or (C) sodium (Na) pyrophosphate during sequential extraction for each fungal isolate (n=4).** Box color represents different fungal species. Individual sample points are shown as dot plots. While a substantial portion of soil C was extracted by water, KCl and sodium pyrophosphate for the two Basidiomycota species (PaS, GyS), for many of the Ascomycota (and to a lesser extent the Mucoromycotina) a significant portion of soil C was unable to be extracted by the three extractants and remained in the soil pellet. This remaining fraction of soil C was termed “chemically stable C” (up to 60% for some species; presented in main text).

Supplementary References

1. Domeignoz-Horta, L. A. *et al.* Direct evidence for the role of microbial community composition in the formation of soil organic matter composition and persistence. *ISME COMMUN.* **1**, 1–4 (2021).
2. Hill, P. W., Farrar, J. F. & Jones, D. L. Decoupling of microbial glucose uptake and mineralization in soil. *Soil Biology and Biochemistry* **40**, 616–624 (2008).
3. Jilling, A., Keiluweit, M., Gutknecht, J. L. M. & Grandy, A. S. Priming mechanisms providing plants and microbes access to mineral-associated organic matter. *Soil Biology and Biochemistry* **158**, 108265 (2021).
4. Kallenbach, C. M., Frey, S. D. & Grandy, A. S. Direct evidence for microbial-derived soil organic matter formation and its ecophysiological controls. *Nature Communications* **7**, 1–10 (2016).
5. Rousk, J. & Bååth, E. Growth of saprotrophic fungi and bacteria in soil. *FEMS Microbiology Ecology* **78**, 17–30 (2011).
6. Jones, D. L. *et al.* Role of substrate supply on microbial carbon use efficiency and its role in interpreting soil microbial community-level physiological profiles (CLPP). *Soil Biology and Biochemistry* **123**, 1–6 (2018).
7. Compton, J. E. & Boone, R. D. Long-Term Impacts of Agriculture on Soil Carbon and Nitrogen in New England Forests. *Ecology* **81**, 2314–2330 (2000).
8. Manzoni, S., Taylor, P., Richter, A., Porporato, A. & Ågren, G. I. Environmental and stoichiometric controls on microbial carbon-use efficiency in soils. *New Phytologist* **196**, 79–91 (2012).

9. Sinsabaugh, R. L. *et al.* Stoichiometry of microbial carbon use efficiency in soils. *Ecological Monographs* **86**, 172–189 (2016).
10. Morrison, E. W. *et al.* Evidence for a genetic basis in functional trait tradeoffs with microbial growth rate but not growth yield. *Soil Biology and Biochemistry* **172**, 108765 (2022).
11. Geyer, K. M., Kyker-Snowman, E., Grandy, A. S. & Frey, S. D. Microbial carbon use efficiency: accounting for population, community, and ecosystem-scale controls over the fate of metabolized organic matter. *Biogeochemistry* **127**, 173–188 (2016).
12. Geyer, K. M., Dijkstra, P., Sinsabaugh, R. & Frey, S. D. Clarifying the interpretation of carbon use efficiency in soil through methods comparison. *Soil Biology and Biochemistry* **128**, 79–88 (2019).